Rapid Viscosity Measurement Using Arbitrary Frequency Magnetic Particle Spectrometer

Haoran Zhang, Bo Zhang, Xin Feng, Yingqian Zhang, Yundai Chen, Hui Hui, *Member, IEEE*, and Jie Tian, *Fellow, IEEE*

***Abstract*— Magnetic particle spectrometer (MPS) is the device for characterizing the properties of magnetic nanoparticle (MNP) suspensions, such as viscosity, temperature, and concentration. Specifically, in viscosity measurement, MPS usually works at one or several fixed frequencies. It is challenging to find the appropriate frequency for viscosity measurement of different MNP suspensions. The frequency parameter can be introduced into the measurement method to improve the measurement accuracy. Here, we developed an arbitrary frequency MPS to measure the harmonic amplitudes of the magnetization signals of MNPs, which were generated at various frequencies. A method of measuring the viscosity of MNP suspensions by harmonic ratios at different frequencies was proposed. The viscosity measurement time used in the experiment is 1 s, and the shortest measurement time available is 0.2 s. Experimental results show that the arbitrary frequency MPS can measure the viscosity of samples ranging from 0.77 mPa·s to 3.87 mPa·s, and the average measurement deviation is 2.7%. The method was validated using plasma samples from normal rabbits and high-fat diet (HFD) rabbits. Normal rabbit measurements differed from the reference by less than 4.5%, and the plasma viscosity of normal and HFD rabbits could be clearly distinguished.**

***Index Terms*— Arbitrary frequency, magnetic nanoparticles (MNPs), magnetic particle spectrometer (MPS), viscosity measurement.**

I. Introduction

MEASUREMENT of the microenvironment in vivo is an important prerequisite for the realization of precision medicine. Among microenvironment parameters, viscosity has important significance in clinical diagnosis and treatment [1]. The accumulation of red blood cells in the circulation leads to an increase in blood viscosity [2]. Whole blood viscosity and plasma viscosity have been shown to have strong connections with disease, including cardiovascular disease (CVD) [3], [4], liver cirrhosis [5], and Alzheimer's disease [6]. Regular measurement of blood viscosity can help detect these conditions in time. In addition to the blood viscosity associated with disease, cancer cells have a higher viscosity than normal cells [7]. Tumor growth can cause oxygen deprivation in tissues, leading to a high viscosity phenomenon [8]. Therefore, tissue viscosity was used for cancer prognoses such as breast cancer [9] and uterine cancer [10].

Due to the strong association between microenvironmental viscosity and disease, accurate viscosity measurements are critical. The current viscosity measurement methods include capillary, falling ball, and oscillatory [11]. Capillary measurement is based on the principle that the viscosity of a liquid in an upright capillary is proportional to the flow time [12]. Capillary cleaning is difficult, and the accuracy of this method is easily affected by the humidity in the viscometer. The falling ball method, which is based on Stoke's principle, is used for the measurement of high viscosity [13]. However, it is necessary to accurately measure the velocity of the ball during the experiment, and the method needs a relatively long time to get the measurement results. Oscillating viscometers require a vibration unit to be placed into a liquid and the attenuation time of the oscillations is used to measure viscosity [14]. This type of viscometer requires prior knowledge of the fluid behavior of the liquid. As discussed, the current common viscosity measurement methods have disadvantages in accuracy and speed.

Magnetic nanoparticles (MNPs) were considered miniature sensors that can achieve precision and speed requirements. This is because the magnetic response of MNPs has been shown to be related to the parameters of the suspension and excitation frequency of the applied magnetic field [15], [16]. In the past decade, MNPs have been widely used as biosensors for quantifying the viscosity through magnetization response signals [17] and for noninvasive imaging of targeted molecules in magnetic particle imaging (MPI) [18], [19]. MNP materials have nonlinear response characteristics, and their response signals are usually transformed to the frequency domain for analysis [20], [21]. It is well known that the magnetic properties of MNPs, such as harmonic spectra and

Manuscript received 10 March 2023; revised 30 June 2023; accepted 4 July 2023. Date of publication 25 July 2023; date of current version 8 August 2023. This work was supported in part by the National Key Research and Development Program of China under Grant 2017YFA0700401; in part by the National Natural Science Foundation of China under Grant 62027901, Grant 81827808, Grant 81227901; the Beijing Natural Science Foundation under Grant JQ22023, 7232346; the Chinese Academy of Sciences Youth Innovation Promotion Association under Grant Y2022055 and Key Technology Talent Program. The Associate Editor coordinating the review process was Dr. Seyed Hossein Hesamedin Sadeghi. *(Corresponding authors: Hui Hui; Jie Tian.)*

Haoran Zhang, Bo Zhang, and Jie Tian are with the School of Engineering Medicine, the School of Biological Science and Medical Engineering, and the Key Laboratory of Big DataBased Precision Medicine, Ministry of Industry and Information Technology of China, Beihang University, Beijing 100191, China (e-mail: hrzhang@buaa.edu.cn; zhangbo1996@buaa.edu.cn; tian@ieee.org).

Xin Feng and Hui Hui are with the CAS Key Laboratory of Molecular Imaging, Institute of Automation, Chinese Academy of Sciences, the Beijing Key Laboratory of Molecular Imaging, and the University of Chinese Academy of Sciences, Beijing 100190, China (e-mail: xin.feng@ia.ac.cn; hui.hui@ia.ac.cn).

Yingqian Zhang and Yundai Chen are with the Senior Department of Cardiology and the Sixth Medical Center of PLA General Hospital, Beijing 100048, China (e-mail: niniya731@163.com; cyundai@vip.163.com).

Digital Object Identifier 10.1109/TIM.2023.3298428

intensity of magnetization, are varying with viscosities [22]. Therefore, by placing MNPs in suspension, the viscosity can be measured by detecting and analyzing the change in the signal.

Magnetic particle spectrometer (MPS) is generally used in the magnetization response analysis of MNPs [23], [24]. Viscosity measurement based on MNPs is generally realized by MPS [25]. However, current MPS operates only at one or several fixed frequencies [26], [27], thus ignoring frequency, an important parameter that affects the magnetization response. Because the optimal frequency for viscosity measurement varies among different types of MNPs, the tuning circuit needs to be redesigned when the operating frequency is changed [28]. To address these issues, we have designed an arbitrary frequency MPS device to generate a sufficient magnetic field without tuning. Magnetic responses of MNPs at different frequencies can be measured. Moreover, the viscosity of MNP suspensions can be accurately measured by utilizing the characteristics of different harmonic signal ratios of MNPs at different viscosities and frequencies. Compared with existing methods, the proposed method based on system functions makes full use of the important parameter of frequency and does not need complex theoretical calculation for the results. Viscosity measurement time is only 1 s. More importantly, by utilizing a convenient measurement, the system functions of a certain type of MNP can be established and used for a long time.

In this article, the theoretical method of viscosity measurement using the relationship between the viscosity and harmonic spectra is first introduced. Then, the design process and structure of arbitrary frequency MPS are introduced in detail. In the experiment, samples of glycerin and gelatin were measured. Two types of MNPs were used in the measurement and their properties for viscosity measurement were investigated. The viscosity can be measured from 0.77 to 3.87 mPa·s, and the average measurement deviation is 2.7%. Besides, to verify that the method and device can be used for an actual medical diagnosis, plasma from normal and high-fat diet (HFD) New Zealand white rabbits was measured. The experimental results show that accurate measurement of viscosity can be achieved and rapid diagnosis of hyperlipidemia can be achieved.

II. Methods

When a dynamic magnetic field is applied to MNPs, the change in the magnetization magnitude of MNPs will occur a little later than the change in the magnetic field strength. This phenomenon is caused by relaxation effects, which is determined by both Brownian and Néel relaxations [29]. The two relaxation phenomena occur simultaneously and dominate at different frequencies. Brownian relaxation dominates at lower magnetic field frequencies, and Neal relaxation gradually dominates with increasing frequency. At frequencies below 2 kHz, Brownian relaxation is more dominant [30]. Viscosity measurements can be made using Brownian relaxation in this frequency range. In addition, the intensity of the two kinds of relaxation phenomena is related to the characteristics of the particles. The Brownian relaxation phenomenon can be better observed by choosing specific particles, and the Brownian relaxation time τ_B is dependent on viscosity in the form

$$\tau_B = \alpha \frac{3\eta V_H}{k_B T} = \frac{1}{\sqrt{1 + 0.126\left(\frac{M_s V \mu_0 H}{k_B T}\right)^{1.72}}} \frac{3\eta V_H}{k_B T} \tag{1}$$

where η is the dynamic viscosity of the solution, V_H is the hydrodynamic particle volume, k_B is the Boltzmann constant, T is the absolute temperature, M_s is the saturation magnetization, V is the volume of each particle, and H is the magnetic field. Therefore, viscosity can be measured by Brownian relaxation time.

The applied magnetic field is generally sinusoidal when MNPs are used for microenvironment detection. The magnetization behavior of MNPs in a sinusoidal magnetic field can be described by the Fokker–Planck equation (FPE) [31]

$$2\frac{\tau^{\mathrm{B}}}{\alpha}\frac{\partial W(\theta,t)}{\partial t} = \frac{1}{\sin\theta}\frac{\partial}{\partial\theta}\left\{\sin\theta\left[\xi\sin\theta\cdot W(\theta,t) + \frac{\partial W(\theta,t)}{\partial\theta}\right]\right\} \tag{2}$$

with

$$\xi = \frac{mH}{k_B T}\cos(\omega t) \tag{3}$$

$$m = \mu_0 M_s V \tag{4}$$

where m is the magnetic moment of MNPs and θ is the angle between m and H. $W(\theta,t)$ is the probability density of the magnetic moment orientations, $\omega = 2\pi f$ with f is the frequency of the exciting magnetic field and μ_0 is the magnetic permeability of free space. Thus, MNP magnetization $M(t)$ can be expressed as follows:

$$M(t) = cM_s\int_{-\pi}^{0}\theta W(\theta,t)\mathrm{d}\theta \tag{5}$$

where c is the MNP concentration. The FPE indicates that the MNP magnetization and the ith harmonic amplitude A_i of the MNP signal depend on $\omega\tau_B$. Thus, A_i depends on the term $f\eta$ when the absolute temperature T, magnetic field H, and the MNP concentration c are constant. This means that the harmonic ratios of the third to the first harmonics and the fifth to the third harmonics are dependent on the term $f\eta$. The relationship between the harmonic ratio, parameter η, and parameter f can be expressed as follows:

$$A_5/A_3 = U(f\eta) \tag{6}$$

$$A_3/A_1 = V(f\eta). \tag{7}$$

Notably, it is difficult to obtain the exact solutions of the two functions $U(f\eta)$ and $V(f\eta)$, and different types of MNPs correspond to different functions. Fortunately, these two functions can be obtained by fixing one parameter and changing another. According to the monotonic property, the two functions can be solved by continuously applying a frequent-changing magnetic field to MNPs with constant viscosity. Then, using these two functions, MNP suspensions with unknown viscosity can be measured at a fixed magnetic field frequency. In addition, the two functions can be obtained at different magnetic field

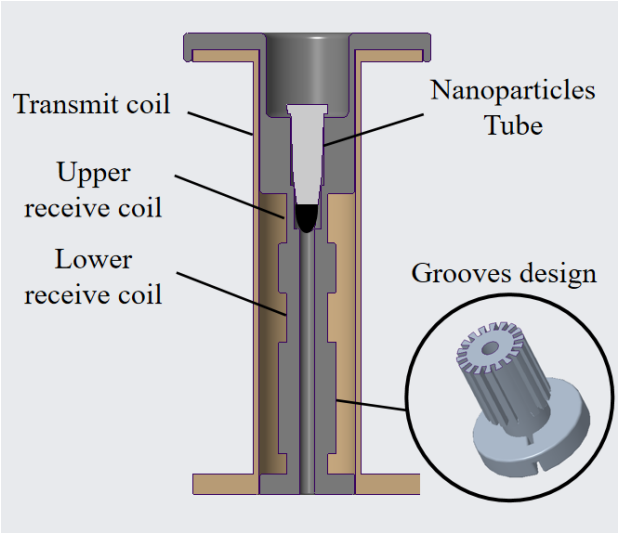

Fig. 1. Design of the arbitrary frequency MPS. A tube containing nanoparticles is placed in the device's coil structure, which contains a transmit coil and a two-part receive coil. Grooves used to improve device performance are zoomed in.

amplitudes, and the viscosity measurements obtained by the functions can be averaged to improve measurement accuracy.

The viscosity of the MNP suspensions used to obtain the two functions is η_0, the minimum frequency used is f_L, and the maximum frequency is f_H. Frequencies are selected at suitable intervals between f_L and f_H, and a sinusoidal magnetic field at these frequencies is applied to the MNP suspensions. Then, using the two functions obtained, the viscosity of other MNP samples can be measured at a fixed frequency $(f_L + f_H)/2$. The viscosity range that can be measured by using this method is (η_L, η_H). Theoretically, the minimum and maximum measurable viscosities (η_L and η_H) can be expressed as follows:

$$\eta_L = \frac{2 f_L \eta_0}{f_L + f_H} \tag{8}$$

$$\eta_H = \frac{2 f_H \eta_0}{f_L + f_H}. \tag{9}$$

The range of viscosities that can be measured can be adjusted by changing the frequencies. It should be noted that different kinds of MNPs used for viscosity measurement will achieve the best measurement results under different conditions. These results are related to particle size and sensitivity to viscosity. Based on the experimental data, suitable magnetic field amplitude and harmonic ratio should be selected for each kind of MNP for viscosity measurement.

III. Design of the Spectrometer

To measure the viscosity of MNP suspensions using the above-mentioned method, the arbitrary frequency MPS was designed, as shown in Fig. 1. In the MPS, MNPs are periodically driven by the sinusoidal magnetic field with sufficiently large amplitudes and multiple frequencies. The corresponding unique magnetic response signals are recorded and decomposed into their spectral components.

A. Transmit and Receive Coil Design

To generate a high magnetic field amplitude, the ac impedance and reactive power of the transmit coil need to be reduced. In common MPS devices, the tuned circuit is used to reduce the impedance of a specific frequency. The MPS is designed to operate over a wide frequency range, reducing the overall impedance by miniaturizing the coil. The sinusoidal magnetic field was generated using a 124-turn solenoidal coil with 100 mm in length and 26 mm in diameter. The length and diameter were chosen to ensure the uniformity of the magnetic field in the sample region. The transmit coil generated a 1.42 mT/A magnetic field with 98% homogeneity within a 12-mm receiving region. The transmit coil was untuned for arbitrary frequencies. The transmit coil can easily generate a magnetic field with an amplitude of 15 mT at a frequency below 3 kHz, which was conducive to viscosity measurements. The impedance of the transmit coil in the 0–3-kHz frequency range is detected and recorded. It is used to determine the voltage that needs to be applied to produce a magnetic field of the same strength at different magnetic field frequencies.

The receive coil was designed with two solenoidal double-layer sections placed coaxially and symmetrically within the transmit coil. The coils in the two sections were wound in reverse. Each section had 100 turns with 12 mm in length and 10 mm in diameter. The coil was made of a 0.2-mm copper wire to improve receiving sensitivity. The upper and lower receive coils were used to measure the MNP signal and to suppress the coupling of the transmit coil, respectively. In practice, the number of turns of the lower section was slightly adjusted to improve the effect of coupling suppression. The interior of the device allows for a nanoparticles tube with a volume of 0.60 mL, and the bottom area of the tube with a volume of 0.15 mL is located inside the upper receive coil.

B. Structure Design

Structural components were designed according to the diameter and length of the transmit coil and receive coils. The outer and inner components were used to wind the transmit and receive coils, respectively. In addition, the inner component was evenly designed with ten grooves at its lower part for fine-tuning the number of turns of the lower receive coil. All the structural components are made by 3-D printing.

C. MPS Setup

Original sinusoidal signals were generated and adjusted by computer control software and data acquisition. Sinusoidal signals with different frequencies were amplified by an AE Techron 7548 power amplifier (AE Techron Inc., USA) and then passed through the transmit coil. The advantage of the MPS device is that there is no need to design tuning circuits for each magnetic field frequency used. The relatively simple circuit structure allows the device to be more portable. The current waveform in the transmit coil was detected in real time by a current sensor. The signal of the MNPs was detected by the receive coil and differentially amplified 100× (SR560, Stanford Research Systems, USA). The final

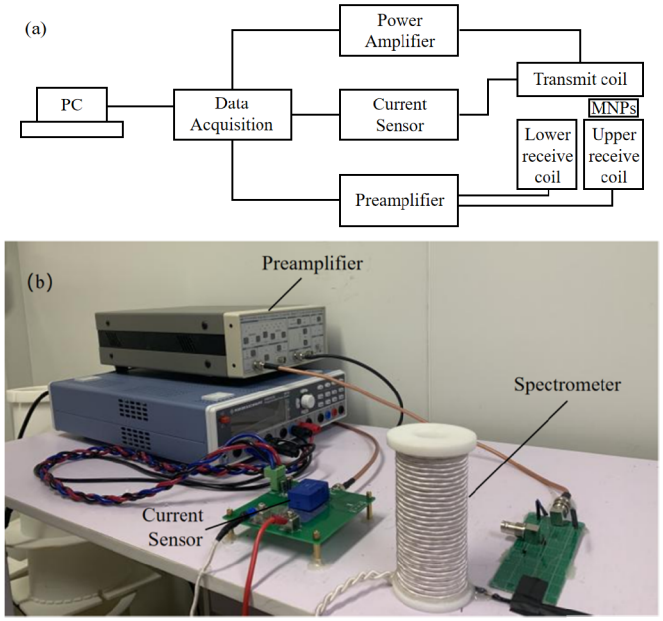

Fig. 2. (a) Schematic and (b) actual photograph of the arbitrary-frequency MPS device.

signal was collected via data acquisition at the sampling rate of 1 MS/s, and the signal was processed by control software. The processing process included background noise reduction, Fourier transform, and digital phase-sensitive detection. The schematic and digital photograph of the developed MPS device are shown in Fig. 2.

The device was set to work in two modes. These two modes correspond to the function acquisition and the viscosity measurement, respectively. The function acquisition mode can be operated continuously after setting the frequency range, frequency interval, and magnetic field amplitude. The device will operate for 1 s at each set frequency, with 1-s intervals between them to ensure device stability. The magnetic field of the device in the aperture direction is shown in Fig. 3. When acquiring the functions, the device needs to run once with and without the standard sample. In data processing, the signal is subtracted under two runs to accurately obtain the response signal of the sample. The viscosity measurement mode can operate stably with a fixed magnetic field amplitude and frequency. The time for viscosity measurement is 1 s. After data acquisition is completed, the viscosity result will be calculated according to the function of the MNPs used. In general, the device is easy to use. It only requires two measurements of the function acquisition mode using standard MNPs samples, and then the sample of unknown viscosity only needs to be measured for 1 s to get the viscosity result. Since the function corresponding to each MNP in this device is relatively fixed, the device only needs to run the function acquisition mode when changing the type of MNPs. Therefore, once a suitable type of MNP is determined, the viscosity measurement time is 1 s.

The transfer function of the device was measured and the signal was calibrated according to the transfer function. The measured transfer function was stored in the software. Before obtaining harmonic ratios, the software processes the

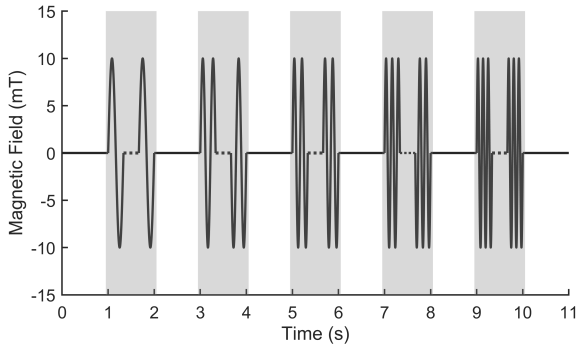

Fig. 3. Magnetic field inside the device in the function acquisition mode. The time for the device to generate sinusoidal magnetic fields of different frequencies is highlighted in gray. The interior of the waveform is omitted appropriately.

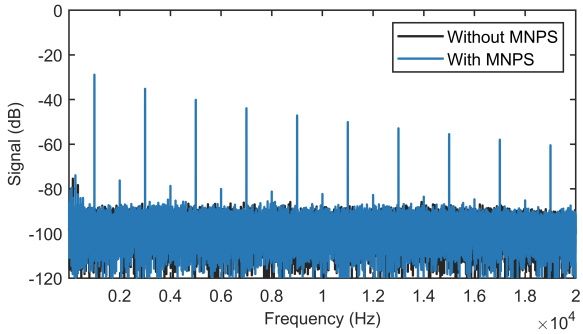

Fig. 4. Spectrum of signals with and without MNPs. The amplitude of the signal at each frequency is expressed in dB.

received signal according to the transfer function. To verify the measurement accuracy, the performance of the device was analyzed. Signals with and without MNPs were recorded, and the signal-to-noise ratio was calculated. The harmonic signals with and without MNPs are shown in Fig. 4. The signals measured without MNPs were about −100 dB at each frequency in the frequency domain. In contrast, signals with MNPs were distributed in the harmonic of the magnetic field frequency in the spectrum. Signals generated by MNP magnetization were shown at odd harmonics, while some even harmonics existed below −85 dB. Even harmonics possibly resulted from the nonlinear distortion of the power amplifier. Nonetheless, noises other than odd harmonics were relatively weak and were filtered out in the subsequent processing and analysis. Besides, noises with the same frequency as odd harmonics were removed by the software. Therefore, the device can accurately obtain the signal of MNPs.

IV. Experimental Results

A. Experimental Description

In this study, two types of MNPs were measured to verify the feasibility of the proposed method: Perimag (Micromod Partikelt-echnologie GmbH, Germany) with hydrodynamic size of 130 nm and iron concentration of 5 mg/mL, and Synomag (Micromod Partikelt-echnologie GmbH, Germany) with hydrodynamic size of 70 nm and iron concentration of 10 mg/mL. The volume and content of the MNPs in each sample remained the same to eliminate the concentration effect.

In glycerol-related experimental samples, 50 μL of MNPs were used in each sample and diluted to a final volume of 150 μL. Solvents with different viscosities were prepared by mixing glycerol and water. By varying the glycerol mass ratios, solvents with six different viscosities were generated: 2%, 10%, 20%, 28%, 36%, and 39%. Samples of Perimag were named Perimag-1 to Perimag-6, and Samples of Synomag were named Synomag-1 to Synomag-6, corresponding to the six different viscosities. To obtain the system functions, samples with the glycerol mass ratio of 28% (Perimag-1 and Synomag-1) were used. The excitation frequencies, ranging from 200 to 1800 Hz, were used in these experiments. The amplitude of the magnetic field is set to three different values. Additional samples, Perimag-2 to Perimag-6 and Synomag-2 to Synomag-6, with glycerol mass ratios of 2%, 10%, 20%, 36%, and 39%, respectively, were used to verify the accuracy of the method for viscosity measurement in a magnetic field with constant frequency and amplitude. The mass ratio of glycerol in the samples is directly related to the viscosities of the samples. 28% of the glycerol mass ratio is determined based on human plasma viscosity, and the other five mass ratios are selected based on the viscosities within the range of measurable viscosity calculated by (8) and (9).

In addition to simulating a viscous environment by mixing glycerol and water, the two types of MNPs described above were used with gelatin to formulate the samples. The harmonic ratios were obtained by using samples of the two types of MNPs with a gelatin weight ratio of 10%. Since gelatin greatly affects the Brownian relaxation of MNPs, the frequency used is increased to ensure that harmonic signals can be detected. The magnetic field frequencies used range from 2.5 to 7.5 kHz, and the magnetic field amplitude is 10 mT.

In addition, rabbit plasma samples were measured to verify the measurement accuracy in real animal samples and the ability to diagnose disease of the method and MPS device. Lipid metabolism and obesity-related disease behaviors in rabbits are similar to those in humans [32], and hyperlipidemia can be induced in rabbits by an HFD [33]. Therefore, New Zealand white rabbits were selected as the experimental animal in this study. Since this viscosity measurement experiment is in vitro, there was no significant damage to the animals except for blood collection. Plasma was measured from three normal rabbits and two HFD rabbits. The volume of each rabbit's plasma sample was 100 μL. To ensure measurement accuracy, the MNPs of Perimag were selected based on previous experiments, and the volume of MNPs used was 50 μL.

B. Experiments to Obtain System Functions

The amplitude of the magnetic field affects the Brownian relaxation time and thus the harmonic ratios. Therefore, studying the influence of the magnetic field amplitude is crucial for determining the amplitude used for viscosity measurement. Samples were excited in the MPS device by a magnetic field with a frequency of 1000 Hz and amplitudes ranging from 1 to 10 mT spaced at 1-mT intervals. Response signals at each amplitude were recorded, signal harmonics were extracted by digital phase-sensitive detection technology, and the A_3/A_1 and A_5/A_3 harmonic ratios were calculated. The curves of the two harmonic ratios of Perimag-1 with magnetic field amplitudes obtained by the above method are shown in Fig. 5. It is shown that the harmonic ratios increase with the magnetic field amplitudes, so the magnetic field amplitude should be kept unchanged when the harmonic amplitude was used to measure viscosity. In addition, the influence of the magnetic field amplitude decreases with the increase of the amplitude. To ensure a high signal-to-noise ratio, magnetic field amplitudes of 5, 8, and 10 mT were used in subsequent experiments.

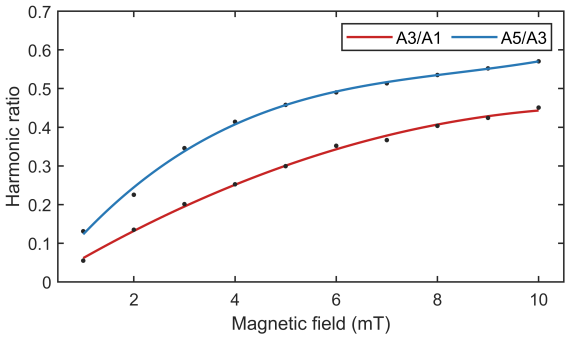

Fig. 5. Relationship between A_3/A_1 and A_5/A_3 harmonic ratios and magnetic field amplitude. The points are experimental data, and the curves act as guides.

Perimag-1 and Synomag-1 were measured at three magnetic field amplitudes with temperatures kept at 20°C, and the sampling rate was 1 MS/s. The two samples were measured using the device's function acquisition mode. The minimum frequency is set to 200 Hz, the maximum frequency to 1800 Hz, and the interval to 50 Hz. The measured signal is transformed into the frequency domain, and the harmonic ratios A_3/A_1 and A_5/A_3 were calculated.

The measurement results of Perimag-1 with magnetic field amplitudes of 5, 8, and 10 mT are shown in Fig. 6. Under different magnetic field amplitudes, the harmonic ratios were obviously different, which was consistent with the previous experimental results. As can be observed in Fig. 6, both harmonic ratios increase with increasing frequency, while the A_5/A_3 ratio exhibited a steep curve while the change in A_3/A_1 was relatively small. Moreover, A_5/A_3 ratios fit well with the least-squares fitting function, while the A_3/A_1 ratios were scattered, which could result from the fundamental frequency component being affected.

Synomag-1 was measured at the same frequency and magnetic field amplitude as described above, and the harmonic ratios were calculated. The experimental results of Synomag-1 are shown in Fig. 7. The A_5/A_3 and A_3/A_1 ratios of Synomag-1 generally decrease with increasing frequency at different magnetic field amplitudes, and the two harmonic ratios increase with increasing magnetic field amplitudes. The harmonic ratios change rapidly in the lower frequency range, while the curve becomes flat at higher frequencies, which is similar to the result of Perimag-1. In addition, the monotonicity of A_3/A_1 is better than that of A_5/A_3. Comparing Fig. 6 with Fig. 7, the change of harmonic ratios shows an inverse trend between Perimag-1 and Synomag-1, which is caused by the intrinsic differences of the two NMPs, including size, shape, and iron core distribution.

To ensure accurate viscosity measurement, harmonic ratio curves should remain monotonous with a sufficient dynamic

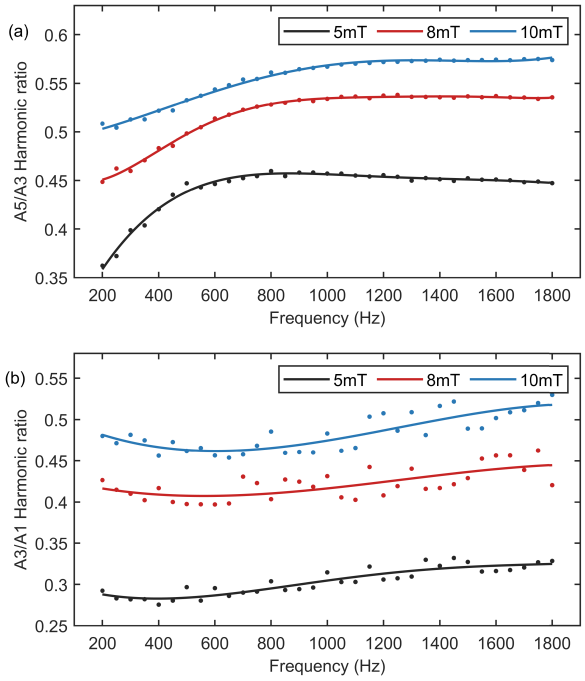

Fig. 6. (a) A_5/A_3 harmonic ratios and (b) A_3/A_1 harmonic ratios of Perimag-1. The points are experimental data, and the curves act as guides.

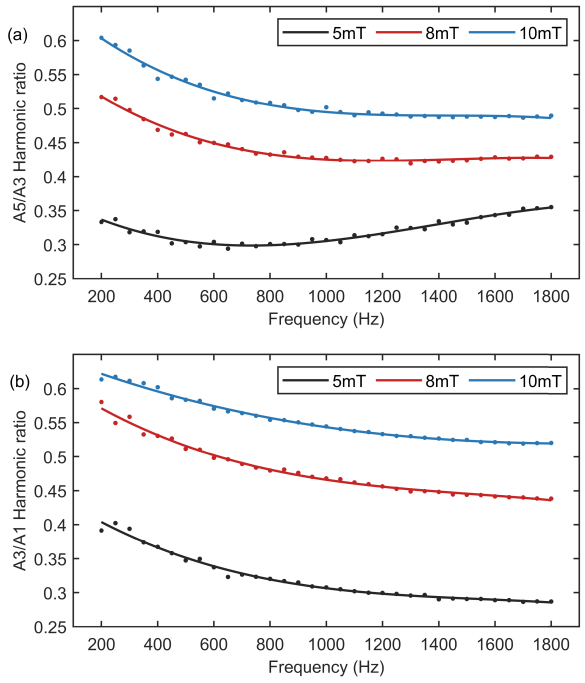

Fig. 7. (a) A_5/A_3 harmonic ratios and (b) A_3/A_1 harmonic ratios of Synomag-1. The points are experimental data, and the curves act as guides.

range. The range of frequencies that satisfies the requirements is directly related to the range of viscosity that can be measured. Therefore, the analysis of alternative frequency ranges is critical. The harmonic ratio curves with good monotone and fitting effect are the A_5/A_3 ratio of Perimag-1 and A_3/A_1 ratio of Synomag-1. The range of frequencies that can be selected is different in the results of the experiment for both ratios. As the magnetic field amplitude increases from 5 to 10 mT, the range of monotonousness in the curves becomes

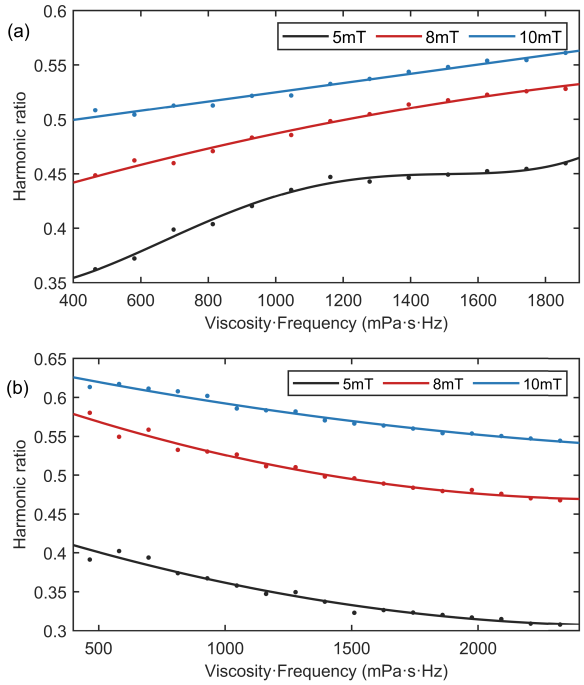

Fig. 8. (a) A_5/A_3 harmonic ratios of Perimag-1 and (b) A_3/A_1 harmonic ratios of Synomag-1 used for viscosity measurements. The points are experimental data, and the curves act as guides.

larger, and the range of frequencies that can be selected becomes larger. Therefore, the viscosity measurement range can be expanded by increasing the magnetic field amplitude, which has a guiding significance for the application of the method. In this study, to use more harmonic ratios at different magnetic field amplitudes to improve measurement accuracy, the frequency range with monotonousness of the curve at 5 mT was selected. The A_5/A_3 curve of Perimag-1 and the A_3/A_1 curve of Synomag-1 satisfied the above requirements at frequencies lower than 800 and 1000 Hz, respectively. With the increase in frequency, Brownian relaxation time increases. At higher frequencies, the suboptimal harmonic ratios are caused by the reduced proportion of Brownian relaxation. When choosing MNPs for measurement, MNPs with stronger Brownian relaxation are more suitable for this method, and MNPs of Synomag have a higher measurement range than that of Perimag in this study.

The A_5/A_3 harmonic ratios of Perimag-1 and A_3/A_1 harmonic ratios of Synomag-1 were analyzed, and the frequency range used for viscosity measurement was 200–800 Hz for Perimag-1 and 200–1000 Hz for Synomag-1. According to reference [34], the viscosity of the 28% glycerol mass ratio (Perimag-1 and Synomag-1) at 20 °C was 2.324 mPa·s. Then, the viscosity was multiplied by the frequency of the magnetic field. The harmonic ratios in the selected frequency range were fit, and the results are shown in Fig. 8.

Frequencies and harmonic ratios of different types of MNPs are different, which is consistent with the purpose of an arbitrary frequency MPS device design. The harmonic ratios of Perimag-1 with magnetic field amplitudes of 8 and 10 mT and the harmonic ratios of Synomag-1 with three magnetic field amplitudes were relatively linear, and the slopes of the fitting curves were also suitable for the measurement of the viscosity

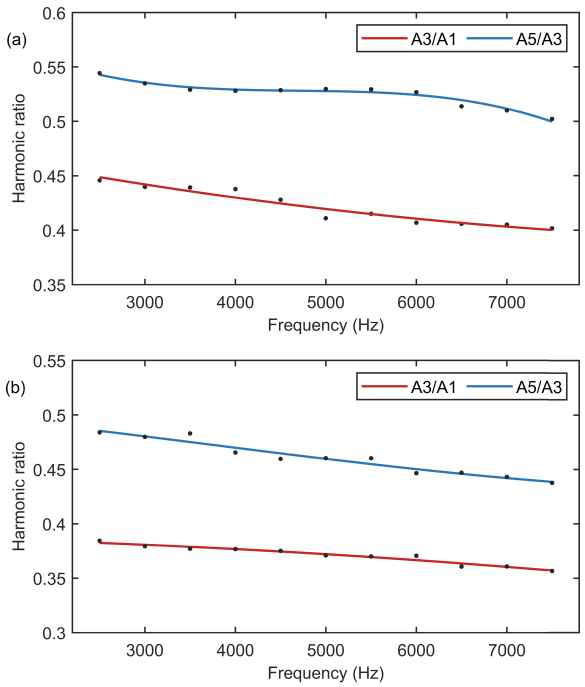

Fig. 9. A_5/A_3 harmonic ratios and A_3/A_1 harmonic ratios of the samples with the gelatin weight ratio of 10%: (a) Harmonic ratios of the Perimag sample and (b) Harmonic ratios of the Synomag sample.

of MNPs. Fig. 8 shows that the multiplications of the viscosity and frequency of two types of MNPs ranged from 464.8 to 1859.2 mPa·s·Hz and 464.8 to 2324.0 mPa·s·Hz. According to (8) and (9), when the Perimag samples were excited with the magnetic field frequency of 500 Hz and the Synomag samples were excited with the magnetic field frequency of 600 Hz, the viscosity ranges measured by the above method were 0.93–3.72 mPa·s and 0.77–3.87 mPa·s, respectively.

In addition to the glycerin samples, the gelatin mixture samples were also measured. The samples with the gelatin weight ratio of 10% were measured at a high-frequency range. The range of 2.5–7.5 kHz is divided into 11 measurement frequencies with intervals of 500 Hz. Response signals of samples with different MNPs were processed, and the harmonic ratios are shown in Fig. 9. The A_5/A_3 harmonic ratios are higher than A_3/A_1 harmonic ratios in both samples at different frequencies, which is the same as the experimental results of the samples with glycerin. The proposed method is proved to be applicable in different viscous environments.

C. Viscosity Measurement Results

To verify the feasibility of this method, Perimag-2 to Perimag-6 and Synomag-2 to Synomag-6 samples were measured with the proposed method and the results were compared with their real viscosities. The samples of Perimag and Synomag were measured in magnetic fields with a frequency of 500 and 600 Hz, respectively. The harmonic ratios of signals were obtained through data processing. The viscosity of ten samples at 20 °C was calculated to obtain the reference viscosity. The measured viscosity results and reference viscosities of these samples are shown in Fig. 10.

The measured viscosity result of different types of MNPs was averaged over the results obtained from the three curves

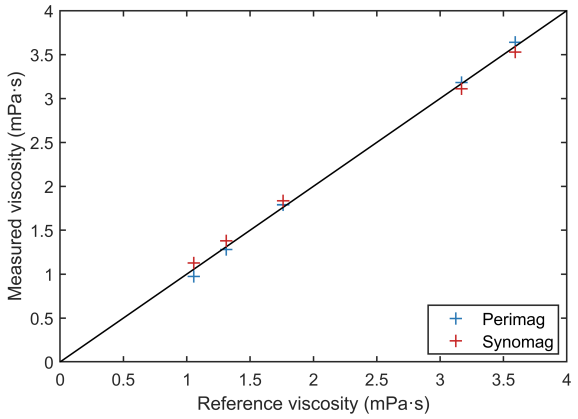

Fig. 10. Comparison of measured viscosity and reference viscosity. The abscissa is the reference viscosity, the ordinate is the viscosity measured using the method, and the diagonal is for comparison purposes.

in Fig. 8. The reference viscosity was obtained using the same method as the viscosity calculation for sample 1. The accuracy of the measurement method can be evaluated by comparing the measured viscosity with the reference viscosity. The reference viscosities of samples 2–6 of the two types of MNPs were 1.055, 1.311, 1.760, 3.169, and 3.593 mPa·s, respectively. The viscosities of samples of Perimag obtained by our method were 0.974, 1.280, 1.792, 3.183, and 3.641 mPa·s, and the viscosities of samples of Synomag obtained by our method were 1.128, 1.380, 1.834, 3.111, and 3.527 mPa·s. In the experiment, the accuracy of viscosity measurement using the two types of MNPs was different. For Perimag, the difference between the measured and reference viscosity was lower than 0.08 mPa·s, with an average deviation of 2.7%. For Synomag, the average deviation was 4.0%. This deviation was caused by the intrinsic properties of different particles and the difference in the degree of harmonic ratio variation within the range of measured viscosity.

Resolutions of viscosity measurements for both types of MNPs were measured. Specifically, the harmonic ratios of MNPs with glycerol ratios of 1% and 2% were measured at a magnetic field amplitude of 10 mT. Results were averaged over five independent measurements. The mean harmonic ratios of Perimag were 0.4993 and 0.5045 with standard deviations of 0.0027 and 0.0032 at 1% and 2% glycerol mass ratios, respectively. The corresponding harmonic ratios of Synomag were 0.6119 and 0.6028, and the standard deviations were 0.0035 and 0.0020, respectively. These demonstrated that the proposed method can resolve viscosity differences as low as 0.026 mPa·s at 20 °C.

The measurement accuracy of this method and device was also verified using real rabbit plasma. Plasma from three normal rabbits was used to verify the accuracy of measurements of real biological samples, and plasma from two HFD rabbits was used to verify the possibility of the method for disease diagnosis. The viscosity measurements using MNPs of Perimag at three magnetic field amplitudes are shown in Fig. 11. Each sample was measured using 100 μL of plasma and 50 μL of MNPs. The average plasma viscosity of normal rabbits measured at three magnetic field intensities was 1.098 mPa·s,

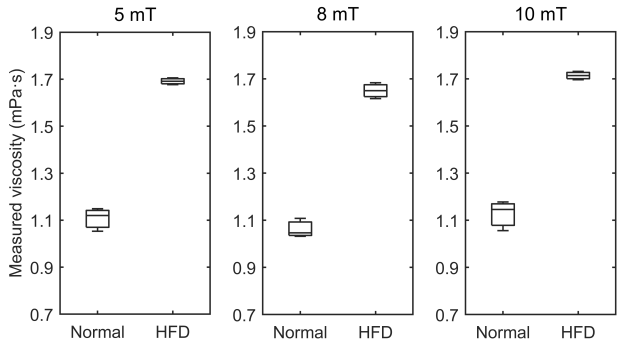

Fig. 11. Plasma viscosity measurements of rabbits on normal and high-fat diets (HFD). From left to right are the viscosities at magnetic field amplitudes of 5, 8, and 10 mT.

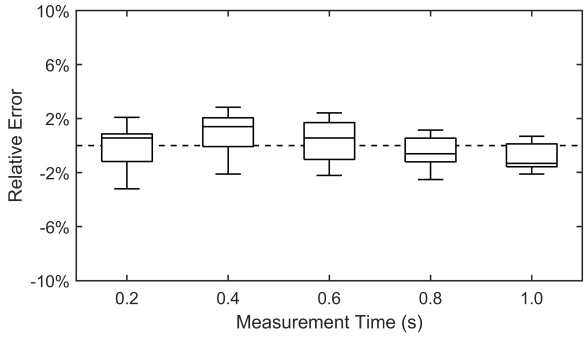

Fig. 12. Relative errors of A_5/A_3 harmonic ratios of Perimag-1 at different measurement times. The dashed line indicates that the relative error is 0%.

which was less than 4.5% difference from that of 30-day-old New Zealand white rabbits in the reference [35]. Because there are differences between individual rabbits, this measurement is considered acceptable. In addition, the results showed that the plasma viscosity of HFD rabbits is significantly different from that of normal rabbits. The mean plasma viscosity measured in HFD rabbits was 1.684 mPa·s. Thus, the measurement accuracy and the possibility of this method and device in disease diagnosis have been proved.

The rapidity of the method and the shortest measurement time available were tested. Since the excitation magnetic field of the device is periodic, the magnetic response signal of MNPs in the sample is periodic. The shortened measurement time reduces the number of periods in the received signal, which does not affect the harmonic ratios. Based on this feature, the measurement times from 0.2 to 1 s were tested with the interval of 0.2 s. The relative errors of A_5/A_3 harmonic ratios of Perimag-1 at different measurement times are shown in Fig. 12. Ten measurements were made at each measurement time. The average value was calculated from all measurements and the relative errors were calculated from this average value. The average errors were calculated separately for each measurement time, and they were less than 1.4% for all five measurement times. As the measurement time decreases, the fluctuation of the harmonic ratio will increase. This is related to the noise signal received by the device. The experiment shows that the minimum measurement time of this method is 0.2 s, but because of the noise signal of the device, the measurement accuracy will be slightly decreased.

V. Discussion

It is demonstrated that the viscosity of two types of MNP suspensions can be measured by the relationship between the harmonic ratio and the product of frequency and viscosity. Moreover, the frequency range suitable for viscosity measurement of different types of MNPs is different, and the measurement accuracy is also different. The results show that MNPs of Perimag have higher accuracy and MNPs of Synomag have a larger range. Accuracy and range are important indicators worth discussing. The accuracy of the measurement can be improved by reducing the frequency interval when obtaining the function. Increasing the number of frequency points helps to better fit the real function. In addition to improving the measurement accuracy from the aspect of function acquisition, when the signal of the viscosity sample is measured, the measurement time can be increased to obtain a more accurate signal spectrum. An accurate spectrum can get a more realistic harmonic ratio. For the range of viscosity that can be measured, it is experimentally confirmed that it can be changed by altering the type of MNPs. When the type of MNPs is fixed, the measurement range can also be improved by increasing the magnetic amplitude. More experiments are needed to find the optimal MNPs suitable for this method.

The experimental results confirm the necessity of using the arbitrary frequency MPS device to measure the viscosity of different types of MNPs. Besides, viscosity in the middle of the measurable range can be accurately measured, with some deviation near the edge of the range. The harmonic ratios of A_5/A_3 and A_3/A_1 are suitable for viscosity measurement of MNPs of Perimag and Synomag, respectively, and the curves obtained by a higher magnetic field amplitude are more linear and monotonous. It is demonstrated that the measurement effect is better by using harmonic ratios of various magnetic field amplitudes. The method can be used for measuring the viscosity in vivo, and the advantage of this method is that different viscosity ranges can be realized by changing parameters μ_0, f_L, and f_H. Experimental results proved that the arbitrary frequency MPS device can accurately measure the harmonic amplitude of the response signal of MNPs. The influence of noise can be significantly suppressed through the design of the receive coil structure and grooves. Since the device allows modification of the frequency and amplitude, the viscosities of different types of MNPs can also be measured.

The solvents of two types of MNPs used in the experiment are phosphate-buffered saline (PBS), which have a density very close to glycerol. The volume of MNPs and their solvent has been taken into account when calculating the volume of glycerin and water required for different viscosities. The effect of MNPs on the viscosity of the sample is weak enough to be ignored. The deviation in the experimental results mainly originates from the inaccurate quality of glycerol and the deviation of temperature. This partly limits this measurement method. The influence of temperature, which is also the main parameter affecting harmonic amplitude, is worth exploring. The measurements of Perimag-1 and Synomag-1 at temperatures of 0 °C, 20 °C, and 50 °C were compared, and the harmonic ratios are shown in Fig. 13. Temperature can affect the harmonic ratios of different types of MNPs at

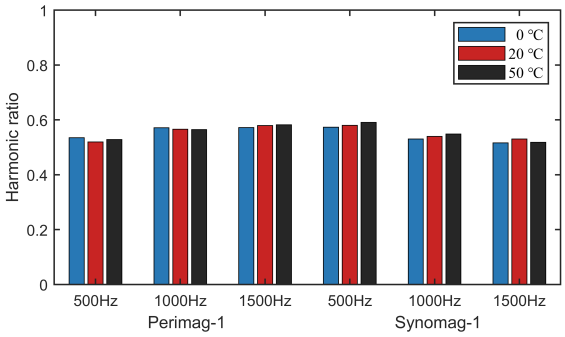

Fig. 13. A_5/A_3 harmonic ratios of samples Perimag-1 and Synomag-1 at three magnetic field frequencies and three temperatures.

different frequencies, which is proved by experimental data. Compared with the effect of viscosity change on harmonic ratios, temperature has a diminished effect, mainly because the relative rate of temperature change is smaller than that of viscosity change. Compared with the harmonic ratio of 20 °C, the change of both samples at 0 °C is more obvious than that at 50 °C. In addition, Perimag-1 was more affected by the temperature with a magnetic field frequency of 500 Hz, while Synomag-1 was more affected by the temperature with a magnetic field frequency of 1500 Hz. Therefore, it is critical to maintain the same temperature when obtaining curves and measuring viscosity. The current measurement process is relatively automated. Sample preparation is manual, while the viscosity measurement process is automatic. When the device completes the measurement without a sample, the user only needs to follow the prompts on the software to put the sample into the device. After placing the sample, the device automatically measures and displays the viscosity result. The measurement is automatic regardless of function acquisition mode at multiple frequencies or viscosity measurement mode at a single frequency.

In future work, this method will be extended to measure the viscosity of a larger range of MNPs using harmonic ratios. Because the device is relatively lightweight in terms of structure, it is possible to be lifted further to reduce the weight and thus achieve a portable device. This will further expand the application prospects of the device.

VI. Conclusion

An arbitrary frequency MPS device to measure the viscosity of different types of MNPs excited at various frequencies and amplitudes has been designed and fabricated. The harmonic ratio method can be applied to accurately measure the viscosities using different MNP samples. The experimental results of glycerin samples and real rabbit plasma samples have validated the proposed method. The viscosity ranges measured using two types of MNPs are 0.93–3.72 and 0.77–3.87 mPa·s, respectively. The measurement errors of the two MNPs are 2.7% and 4%, respectively. Different measurement times were tested, and the relative error of the results for each measurement time is less than 1.4%. The minimum measurement time achieved by this method is 0.2 s. This arbitrary frequency MPS device has the potential to be used in a wide variety of biosensing applications.

Acknowledgment

The authors would like to acknowledge the instrumental and technical support of the Multimodal Biomedical Imaging Experimental Platform, Institute of Automation, Chinese Academy of Sciences.

References

[1] K. Wu, D. Su, J. Liu, R. Saha, and J.-P. Wang, "Magnetic nanoparticles in nanomedicine: A review of recent advances," *Nanotechnology*, vol. 30, no. 50, Dec. 2019, Art. no. 502003.

[2] U. Windberger, A. Bartholovitsch, R. Plasenzotti, K. J. Korak, and G. Heinze, "Whole blood viscosity, plasma viscosity and erythrocyte aggregation in nine mammalian species: Reference values and comparison of data," *Exp. Physiol.*, vol. 88, no. 3, pp. 431–440, May 2003.

[3] S. A. Peters, M. Woodward, A. Rumley, H. D. Tunstall-Pedoe, and G. D. Lowe, "Plasma and blood viscosity in the prediction of cardiovascular disease and mortality in the Scottish Heart Health Extended Cohort Study," *Eur. J. Preventive Cardiol.*, vol. 24, no. 2, pp. 161–167, Jan. 2017.

[4] T. Celik, S. Balta, C. Ozturk, and A. Iyisoy, "Whole blood viscosity and cardiovascular diseases: A forgotten old player of the game," *Med. Princ. Pract.*, vol. 25, no. 5, pp. 499–500, 2016.

[5] C. A. S. Aldana et al., "Hemorheological and biochemical study in patients with liver cirrhosis," *Phys. Fluids*, vol. 34, no. 4, Apr. 2022, Art. no. 041907.

[6] M. M. Smith, P. C. Y. Chen, C.-S. Li, S. Ramanujam, and A. T. W. Cheung, "Whole blood viscosity and microvascular abnormalities in Alzheimer's disease," *Clin. Hemorheol. Microcirculat.*, vol. 41, no. 4, pp. 229–239, 2009.

[7] Y. Wu et al., "A mitochondria targetable and viscosity sensitive fluorescent probe and its applications for distinguishing cancerous cells," *Dyes Pigments*, vol. 168, pp. 134–139, Sep. 2019.

[8] N. C. Denko and A. J. Giaccia, "Tumor hypoxia, the physiological link between Trousseau's syndrome (carcinoma-induced coagulopathy) and metastasis," *Cancer Res.*, vol. 61, no. 3, pp. 795–798, 2001.

[9] G.-F. von Tempelhoff, N. Schönmann, L. Heilmann, K. Pollow, and G. Hommel, "Prognostic role of plasmaviscosity in breast cancer," *Clin. Hemorheol. Microcirculat.*, vol. 26, no. 1, pp. 55–61, 2002.

[10] G.-F. von Tempelhoff, L. Heilmann, K. Pollow, and G. Hommel, "Monitoring of rheologic variables during postoperative high-dose brachytherapy for uterine cancer," *Clin. Appl. Thrombosis/Hemostasis*, vol. 10, no. 3, pp. 239–248, Jul. 2004.

[11] P. Singh, K. Sharma, I. Puchades, and P. B. Agarwal, "A comprehensive review on MEMS-based viscometers," *Sens. Actuators A, Phys.*, vol. 338, May 2022, Art. no. 113456.

[12] Y. Fujita, Y. Kurano, and K. Fujii, "Evaluation of uncertainty in viscosity measurements by capillary master viscometers," *Metrologia*, vol. 46, no. 3, pp. 237–248, Jun. 2009.

[13] T. Lommatzsch, M. Megharfi, E. Mahe, and E. Devin, "Conceptual study of an absolute falling-ball viscometer," *Metrologia*, vol. 38, no. 6, pp. 531–534, Dec. 2001.

[14] T. Voglhuber-Brunnmaier, A. O. Niedermayer, F. Feichtinger, and B. Jakoby, "Fluid sensing using quartz tuning forks—Measurement technology and applications," *Sensors*, vol. 19, no. 10, p. 2336, May 2019.

[15] A. M. Rauwerdink and J. B. Weaver, "Viscous effects on nanoparticle magnetization harmonics," *J. Magn. Magn. Mater.*, vol. 322, no. 6, pp. 609–613, Mar. 2010.

[16] C. Shasha and K. M. Krishnan, "Nonequilibrium dynamics of magnetic nanoparticles with applications in biomedicine," *Adv. Mater.*, vol. 33, no. 23, Jun. 2021, Art. no. 1904131.

[17] M. A. Martens et al., "Modeling the Brownian relaxation of nanoparticle ferrofluids: Comparison with experiment," *Med. Phys.*, vol. 40, no. 2, Jan. 2013, Art. no. 022303.

[18] B. Gleich and J. Weizenecker, "Tomographic imaging using the nonlinear response of magnetic particles," *Nature*, vol. 435, no. 7046, pp. 1214–1217, Jun. 2005.

[19] Y. Li et al., "Modified Jiles–Atherton model for dynamic magnetization in x-space magnetic particle imaging," *IEEE Trans. Biomed. Eng.*, vol. 70, no. 7, pp. 2035–2045, Jul. 2023.

[20] T. Knopp, N. Gdaniec, and M. Möddel, "Magnetic particle imaging: From proof of principle to preclinical applications," *Phys. Med. Biol.*, vol. 62, no. 14, pp. R124–R178, Jun. 2017.

[21] Y. Liu et al., "Weighted sum of harmonic signals for direct imaging in magnetic particle imaging," *Phys. Med. Biol.*, vol. 68, no. 1, Jan. 2023, Art. no. 015018.
[22] D. B. Reeves and J. B. Weaver, "Simulations of magnetic nanoparticle Brownian motion," *J. Appl. Phys.*, vol. 112, no. 12, Dec. 2012, Art. no. 124311.
[23] S. Biederer et al., "Magnetization response spectroscopy of superparamagnetic nanoparticles for magnetic particle imaging," *J. Phys. D, Appl. Phys.*, vol. 42, no. 20, Oct. 2009, Art. no. 205007.
[24] N. Garraud, R. Dhavalikar, L. Maldonado-Camargo, D. P. Arnold, and C. Rinaldi, "Design and validation of magnetic particle spectrometer for characterization of magnetic nanoparticle relaxation dynamics," *AIP Adv.*, vol. 7, no. 5, May 2017, Art. no. 056730.
[25] M. Möddel, C. Meins, J. Dieckhoff, and T. Knopp, "Viscosity quantification using multi-contrast magnetic particle imaging," *New J. Phys.*, vol. 20, no. 8, Aug. 2018, Art. no. 083001.
[26] K. Wu, J. Liu, Y. Wang, C. Ye, Y. Feng, and J.-P. Wang, "Superparamagnetic nanoparticle-based viscosity test," *Appl. Phys. Lett.*, vol. 107, no. 5, Aug. 2015, Art. no. 053701.
[27] M. Utkur, Y. Muslu, and E. U. Saritas, "Relaxation-based viscosity mapping for magnetic particle imaging," *Phys. Med. Biol.*, vol. 62, no. 9, pp. 3422–3439, May 2017.
[28] A. Behrends, M. Graeser, and T. M. Buzug, "Introducing a frequency-tunable magnetic particle spectrometer," *Current Directions Biomed. Eng.*, vol. 1, no. 1, pp. 249–253, Sep. 2015.
[29] J. Dieckhoff, D. Eberbeck, M. Schilling, and F. Ludwig, "Magnetic-field dependence of Brownian and Néel relaxation times," *J. Appl. Phys.*, vol. 119, no. 4, Jan. 2016, Art. no. 043903.
[30] S. Ota and Y. Takemura, "Characterization of Néel and Brownian relaxations isolated from complex dynamics influenced by dipole interactions in magnetic nanoparticles," *J. Phys. Chem. C*, vol. 123, no. 47, pp. 28859–28866, Nov. 2019.
[31] T. Yoshida and K. Enpuku, "Simulation and quantitative clarification of AC susceptibility of magnetic fluid in nonlinear Brownian relaxation region," *Jpn. J. Appl. Phys.*, vol. 48, no. 12R, Dec. 2009, Art. no. 127002.
[32] X.-J. Zhang, D. L. Chinkes, A. Aarsland, D. N. Herndon, and R. R. Wolfe, "Lipid metabolism in diet-induced obese rabbits is similar to that of obese humans," *J. Nutrition*, vol. 138, no. 3, pp. 515–518, Mar. 2008.
[33] Z. Guo et al., "High fat diet–induced hyperlipidemia and tissue steatosis in rabbits through modulating ileal microbiota," *Appl. Microbiol. Biotechnol.*, vol. 106, no. 21, pp. 7187–7207, Nov. 2022.
[34] M. L. Sheely, "Glycerol viscosity tables," *Ind. Eng. Chem.*, vol. 24, no. 9, pp. 1060–1064, Sep. 1932.
[35] U. Windberger, K. Grohmann, A. Goll, R. Plasenzotti, and U. Losert, "Fetal and juvenile animal hemorheology," *Clin. Hemorheol. Microcirculat.*, vol. 32, no. 3, pp. 191–197, 2005.

Haoran Zhang received the B.S. degree in automation from the Civil Aviation University of China, Tianjin, China, in 2020. He is currently pursuing the Ph.D. degree in biomedical engineering with Beihang University, Beijing, China.

His current research interest is microenvironment detection based on magnetic nanoparticles.

Bo Zhang received the B.S. degree in mechanical design manufacturing and automation from Northeast Agricultural University, Harbin, China, in 2018, and the M.S. degree from Northwest A&F University, Xianyang, China, in 2021. He is currently pursuing the Ph.D. degree in electronic information with Beihang University, Beijing, China.

His current research interests include the development of magnetic particle imaging systems and image reconstruction.

Xin Feng received the B.S. degree in biochemistry from China Agricultural University, Beijing, China, in 2011, and the Ph.D. degree in physics and medical physics from the University of Massachusetts Lowell, Lowell, MA, USA, in 2018.

She joined the CAS Key Laboratory of Molecular Imaging, Beijing, in 2020. Currently, she is an Assistant Professor at the Institute of Automation, Chinese Academy of Sciences, Beijing. Her current research interests focus on the hardware design and applications of magnetic particle spectroscopy and magnetic particle imaging.

Yingqian Zhang received the B.M. degree from Shandong University, Jinan, China, in 2011, and the M.D. degree from the Medical School of Chinese PLA, Beijing, China, in 2016.

She joined the Chinese PLA General Hospital, in 2016, where she is currently a Senior Physician at the Senior Department of Cardiology. Her work focuses on interventional treatment of coronary heart disease and valvular heart disease.

Yundai Chen received the B.M. and M.M. degrees from Dalian Medical University, Dalian, China, in 1990 and 1993, respectively, and the M.D. degree from Capital Medical University, Beijing, China, in 2003.

She joined the Chinese PLA General Hospital, Beijing, in 2008, where she is the Director at the Senior Department of Cardiology. She specializes in the interventional treatment of complex coronary heart disease.

Hui Hui (Member, IEEE) received the B.S. and M.S. degrees in mechanical engineering from Chang'an University, Xi'an, China, in 2003 and 2006, respectively, and the Ph.D. degree in mechanical engineering from the University of Franche-Comté, Besançon, France, in 2013.

He is currently a Professor of Institute of Automation, Chinese Academy of Sciences. He is a outstanding member of the Youth Innovation Promotion Association of the Chinese Academy of Sciences. His current research interests include multimodal molecular imaging, magnetic particle imaging, and artificial intelligence medical image processing.

Jie Tian (Fellow, IEEE) received the Ph.D. degree (Hons.) in artificial intelligence from the Chinese Academy of Sciences, Beijing, China, in 1993.

Since 1997, he has been a Professor with the Chinese Academy of Sciences. He is recognized as a Pioneer and the Leader in China in the field of molecular imaging. His current research focuses on molecular imaging and radiomics.

Dr. Tian has been elected as a fellow of ISMRM, AIMBE, IAMBE, OSA, SPIE, and IAPR.